Unsteady RANS simulation of a flow past a free-surface piercing circular cylinder

Maïté Gouin*, Adrien Doradoux*, and Ronan Le Creurer†
* SIREHNA, Bouguenais/France, †Naval Group, Lorient/France
maite.gouin@sirehna.com

1 Introduction

The stealth of submarines is one of the main performance criteria. One important indiscretion source is due to wakes generated by submarine masts when operating at periscope depth. In this work we are interested in the wake generated by a cylindrical mast with a circular cross-section.
The flow around a circular cylinder is characterized by the development of complex free-surface deformations. For submarine cylindrical masts, typical Reynolds numbers are around 10^5 to 10^6 - falling into the critical to supercritical region - and thus making difficult the correct prediction of the drag coefficient [1]. Indeed, in this region, the drag coefficient is decreasing suddenly while increasing the Re number. When dealing with submarine masts, Froude numbers are around 1 to 4, leading to some characteristic behaviours, depending on the Froude numbers [2]. Thus, the numerical modelling of such flows is quite challenging and it has been for a long time a subject of theoretical and analytical research in the naval hydrodynamic field.
Both experimental works ([2][3][4]) and numerical studies (described hereafter) have been conducted to solve this complex problem. First of all, for the case of single phase flows, in [5] the authors compared URANS and DES turbulence modelling at $Re = 9.3\ 10^4$ and $Re = 5.5\ 10^5$ without correctly reproducing the drag coefficient drop. In [6] the authors performed single phase LES simulations in the subcritical to supercritical regimes and obtained the expected drag coefficient drop. Other authors consider a cylinder piercing a free surface ([7][8][9]). In [7] LES simulations were conducted for different Re and Fr numbers with constant ratio Re/Fr, showing the quite correct prediction of the drag coefficient and of the free-surface deformation. The authors in [9] used a RANS modelling of the turbulence and found that RANS studies are accurate enough to capture the free surface elevation.
A RANS modelling approach appears to be sufficient (to correctly reproduce the free surface elevation) and is thus adopted. The interesting quantities are mainly the free-surface deformation in front of the cylinder (bow wave height) and behind the cylinder (trough depth), as well as the cylinder wake. The forces exerted on the cylinder are also of great interest.

2 Numerical method

2.1 Method

A numerical approach using the open source finite volume computational fluid dynamics (CFD) package OpenFOAM v17.12 [10] is used to simulate the incompressible flow past a vertical circular cylinder piercing the free-surface. The URANS simulations use the interFoam solver with a kω-SST turbulence modelling. Turbulence parameters are chosen according to [11]. The PISO algorithm is used with an adjusted time step leading to a Courant number lower than 1 (leading to time steps around $1e10^{-4}$). A target of y+=0.5 is used so that no wall function is employed. The air-water interface is tracked using a Volume Of Fluid (VOF) method with interface recompression.

2.2 Numerical domain

The numerical domain is constructed as follows: in the horizontal plane, it contains 25D upstream, 60D downstream and 50D in the transverse direction. Moreover, for Froude number higher than 2, an extrusion zone is used at the outlet of the domain to damp the created wake. In the vertical direction, it contains 10 cylinder diameters below the free-surface and 5 diameters above. Simulations are run for 2Tref, where Tref = (25+1+60)D/U is the time taken by the flow to cross the domain.

2.3 Mesh

The mesh is generated with the inbuilt OpenFOAM meshing software blockMesh. A boundary layer mesh with y+=0.5 is used along with a fine discretization around the cylinder, as presented in Fig. 1. A mesh convergence has been performed on the first case (Re=234000 and Fr=0.84) to ensure that the main quantities (Cd, bow wave height and trough depth) have converged while refining in the z-direction (assuming that the refinement in the x-direction and y-direction is sufficient). For this case (Re=234000 and Fr=0.84), the mesh consists of 12M of cells.

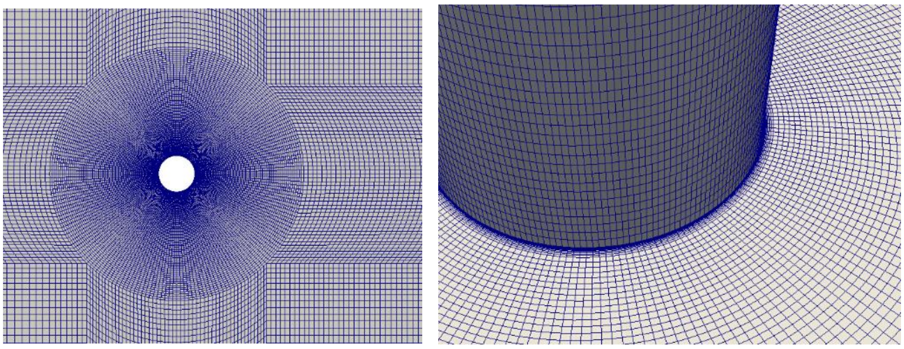

Fig. 1 : Mesh of the computational domain for Re=234000 and Fr=0.84.

2.4 Computed cases

Four operating conditions have been simulated: the case with D=0.2m and V=2.3kts (leading to Re=234000 and Fr=0.8). This case is compared to the experimental data of [2] and the numerical results of [7]. A second case with a higher Froude number Fr=2 and the same Reynolds number Re=234000 is then computed to investigate the effect of a higher Froude number. Then, the effect of a higher Reynolds number is performed with Re=458000 and Fr=0.84. Finally, the effect of a higher velocity on the free-surface deformation with the same diameter as the first case is computed: D=0.2m and V=6kts (Re=614000 and Fr=2.21).

3 Results

3.1 Re=234000 and Fr=0.84 – Validation case

A first simulation is carried out with Re=234000 - Fr=0.84. This first simulation aims at validating the method. The free-surface deformation on the whole domain and close to the mast is presented in Fig. 2 and Fig 3. A good agreement is found with the numerical results of [7]. A synthetic comparison with experimental result [2] and numerical simulation [7] is given in Table 1. The bow wave in front of the cylinder is well reproduced as well as the Kelvin wake angle. The trough depth behind the cylinder is slightly overestimated in our simulation. For this case, free-surface results are in good agreement with the available data.

The mean drag coefficient is also given in Table 1. The OpenFOAM simulation slightly over-predicts the mean drag coefficient compared to the LES simulations of [7]. Moreover, compared to the experimental data of [2], the drag coefficient is much smaller than the biphasic value (1.05). In order to go deeper, the vertical profile of the Cd coefficient is given in Fig 3 and compared to experimental data of [2] and LES simulation of Koo et al. [7]. Our simulation gives a reasonably good prediction of the drag coefficient far from the free surface but does not reproduce the drag coefficient bump close to the free surface, maybe due to the RANS method used. We can observe that the LES simulations of Koo et al. [7] gives a better prediction of the drag coefficient close to the air-water interface.

Table 1 : Results for Re=234000 and Fr=0.84. FS: free-surface. SP: single phase.

Re=234000 Fr=0.84	**Theory**	**Chaplin et Teigen [2]**	**Koo et al. (2014) [7]**	**Simulation**
Bow wave height (/D)	0.35 (Bernoulli)	0.35	0.33	0.34
Trough depth (/D)	0.20 (empirical [12])	0.2	0.24	0.24
Kelvin wake angle	19.5	18-19	18-19	18-19
Cd	-	1.05 FS and 0.75 SP	0.72	0.64
St	-	0.2 Schewe (1983) [13]	0.21	0.26

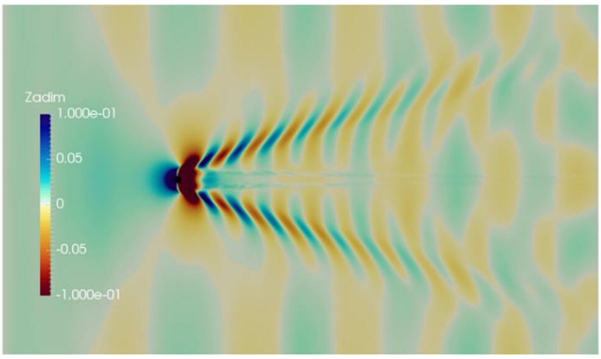

Fig. 2: Free surface elevation (from above). Re=234000 and Fr=0.84.

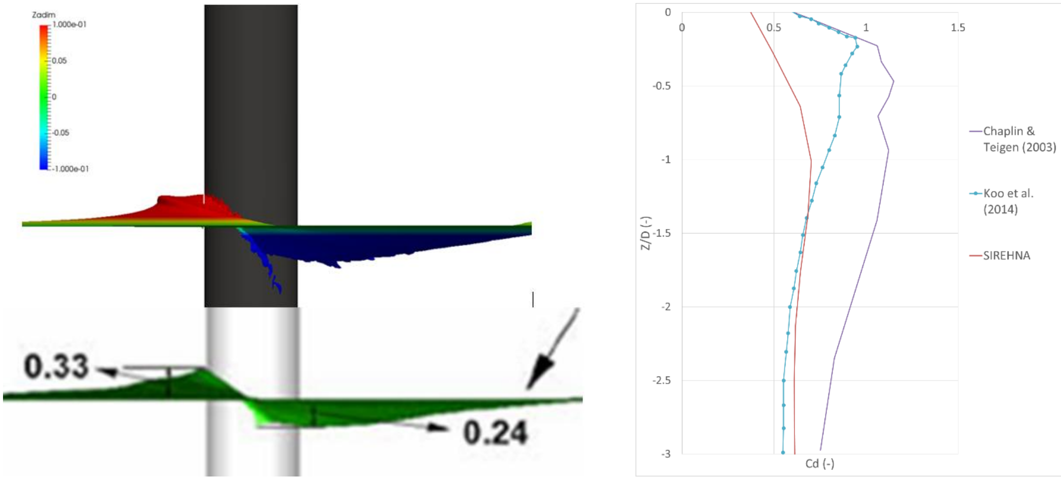

Fig 3: Re=234000 and Fr=0.84. Left: Free surface elevation close to the mast (Above: our result. Below: Results from [7]). Right: Vertical profile of the drag coefficient. Purple: experimental data from [2]. Blue: LES simulation from [7]. Red: Our simulation.

3.2 Re=234000 and Fr=2

This second case investigates the effect of a higher Froude number and the ability of the method to correctly reproduce the main free-surface and force parameters.

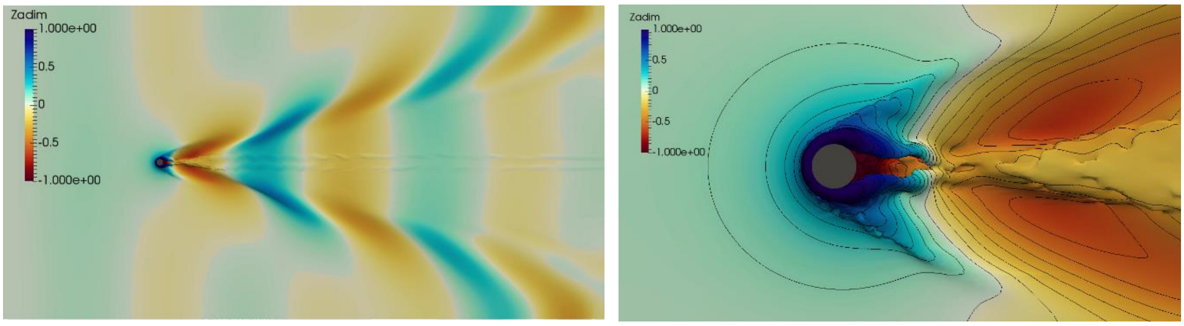

Fig 4: Free surface elevation (from above). Re=234000 and Fr=2.

Table 2: Results for Re=234000 and Fr=2. SP: single phase.

Re=234000 Fr=2	Reference	Simulation
Bow wave height (/D)	2.0 (Bernoulli) and 1.8 (exp [14])	1.6
Trough depth (/D)	1.14 (anal. [12])	1.3
Kelvin wake angle	< 19°	17°
Cd	SP: 0.9	0.55
St	-	0.24

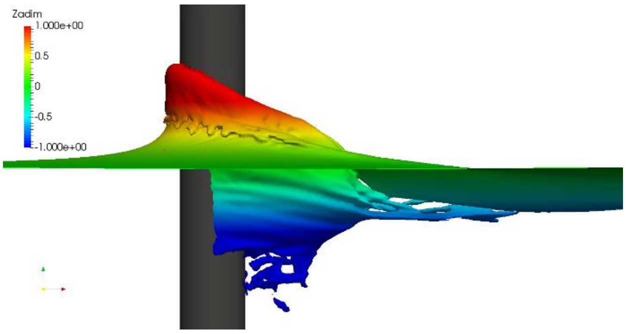

Fig 5: Free surface elevation close to the mast. Re=234000 and Fr=2.

3.3 Re=458000 and Fr=0.84

This third case investigates the effect of a higher Reynolds number. Results are compared to numerical simulations performed by Koo et al.[7].

The free surface elevation is presented on Fig 6 and characteristics parameters are given in Table 3. The free surface elevation is similar to the case Re=234000 and the same Froude number Fr=0.84. Bow wave height and trough depth given by the simulation are very similar to the LES results of Koo et al. [7] (see Fig 7).

Table 3: Results for Re=458000 and Fr=0.84.

	Reference	**Simulation**	**Koo et al. (2014)** [7]
Bow wave height (/D)	0.35 (Bernoulli)	0.35	0.35
Trough depth (/D)	0.2 (anal. [12])	0.25	0.246
Kelvin wavelength (/D)	4.43	4.8	4.35
Cd	0.2 (infinite)	0.56	
St	0.4/0.5	0.39	

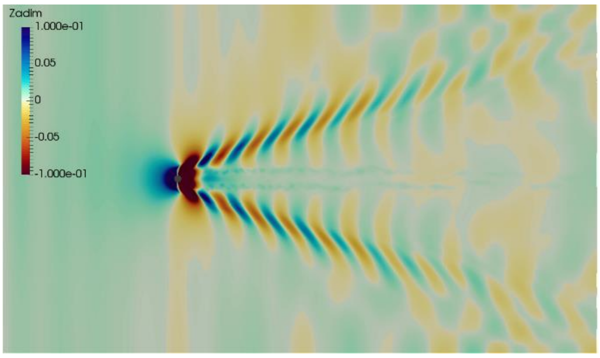

Fig 6: Free surface elevation. Re=458000 and Fr=0.84.

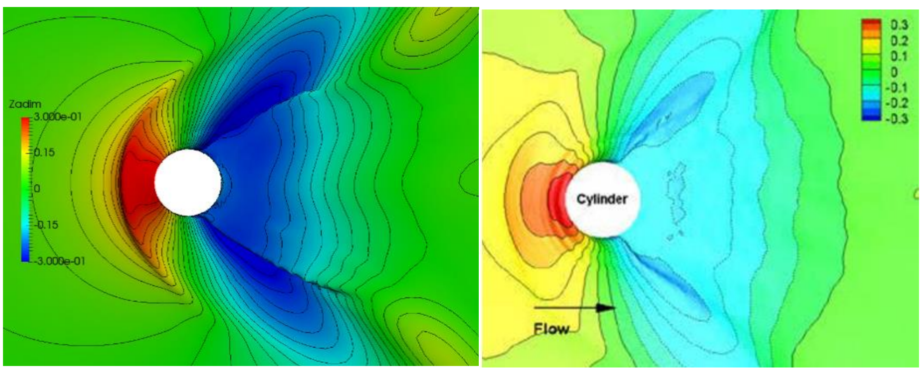

Fig 7: Free surface elevation. Re=458000 and Fr=0.84. Left: OpenFOAM. Right: Results from Koo et al. [7].

3.4 Re=614000 and Fr=2.21

A last simulation is performed with Re=614000 and Fr=2.21 to investigate the effect of a higher mast speed with the same diameter as the first case (D=0.2m). The mesh contains 18 M of cells. The free-surface deformation over the whole domain and close to the mast is presented in Fig 8. The bow wave in front of the cylinder is well reproduced (cf Table 4). The trough depth behind the cylinder is underestimated in our simulation, but it has been reported that it can depart from the analytical formula given in [12] for high values of Re and Fr [2].

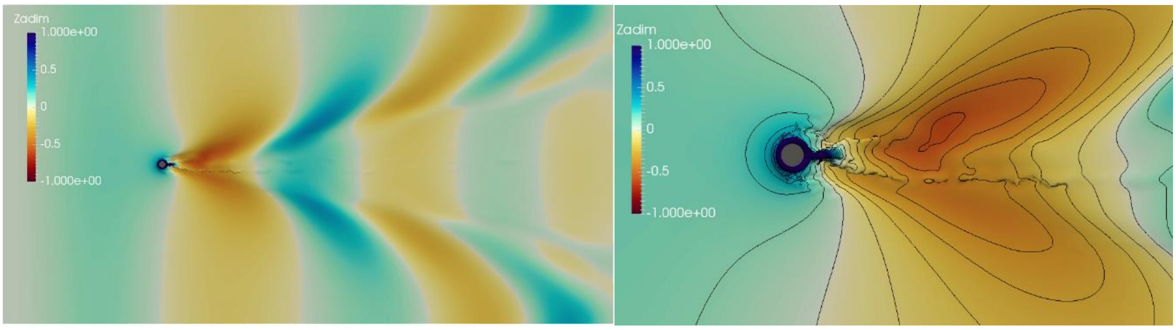

Fig 8: Free surface elevation (from above). Re=614000 and Fr=2.21.

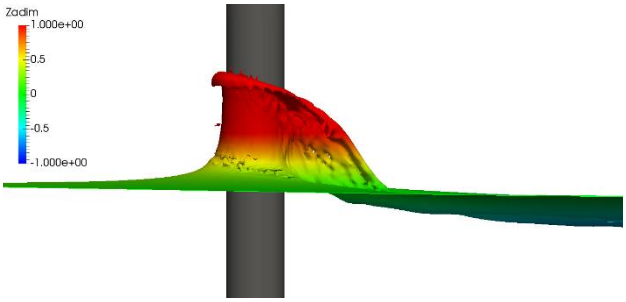

Fig 9: Free surface elevation close to the mast. Re=614000 and Fr=2.21.

Table 4: Results for Re=614000 and Fr=2.21.

	Reference	**Simulation**
Bow wave height (/D)	2.44 (Bernoulli)	2.06
Trough depth (/D)	1.4 (anal. [12])	0.63
Kelvin wake angle	< 19°	16°
Cd		0.56
St		0.24

3.5 CPU time

All computed cases were run on 8 nodes, each node having 20 cores. The summary of CPU time for 10 computed time-steps on 160 cores is reported in Table 5.

Table 5: Summary of CPU time and mesh size.

Computed case	**CPU time for 10 time steps (s)**	**Mesh size (M=millions of cells)**
Re=234000 Fr=0.84	1.9	12 M
Re=234000 Fr=2	4.3	17 M
Re=458000 Fr=0.84	2.7	14.3 M
Re=614000 Fr=2.21	4.2	18.4 M

Thus it appears that the CPU time per timestep is almost linear with the total number of cells. However, the total CPU time depends on both the number of cells and the ratio Re/Fr (as the time step decreases while increasing the Froude number).

4 Conclusion and perspectives

The numerical simulation of a circular mast piercing the free-surface has been presented for different Reynolds and Froude numbers. The main conclusions regarding the physical aspects are the following:

- The free-surface parameters are correctly reproduced by the numerical method (in terms of bow wave height, trough depth (see Fig. 10) and wake),
- The correct modelling of the forces acting on the cylinder is still a challenging task.

Thus the use of a URANS method with a kw-SST model appears to be sufficient to correctly reproduce the free-surface deformation, but the correct modelling of the forces exerted on the cylinder needs more investigation.

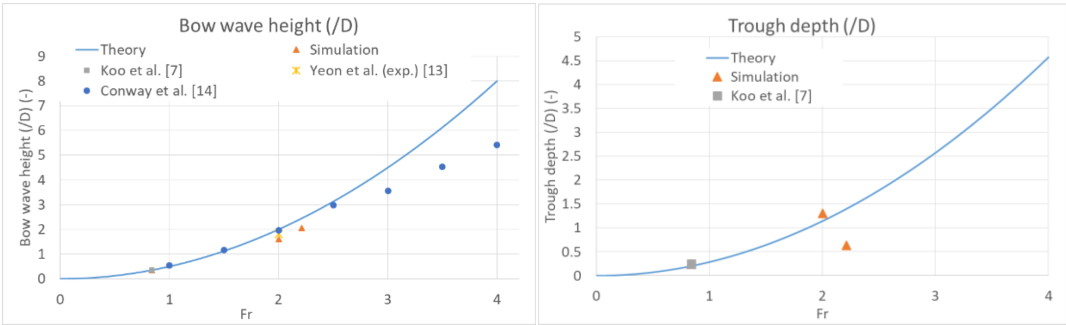

Fig 10: Bow wave height and through depth with increasing Froude number.

References

[1] E. Achenbach, Influence of surface roughness of the cross-flow around a circular cylinder, J. Fluid Mech. 46 (1971) pp321-335.

[2] J.R. Chaplin, P. Teigen, Steady flow past a vertical surface-piercing circular cylinder, Journal of Fluids and Structure 18, 2003, pp271-285.

[3] AST Conway, D. Ranmuthugala, J.R. Binns, M. Renilson, Journal of Engineering for the maritime environment, 2017, pp1-13. The effect of geometry on the surface waves generated by vertical surface-piercing cylinders with a horizontal velocity.

[4] M. Inoue, N. Bara, Y. Himeno, Journal of the Kansai Society of Naval Architects, Japan 220, 1993, pp57-64. Experimental and numerical study of viscous flow field around an advancing vertical circular cylinder piercing a free-surface.

[5] G. Vaz, C. Mabilat, R. van der Wal, P. Gallagher, Proceedings of OMAE, June 10-15, 2007, San Diego, California, USA. Viscous flow around computations on smooth cylinders: A detailed numerical study with validation.

[6] S M Yeon, J. Wang, F. Stern, Applied Ocean Research 59, 2016, pp 663-675. Large Eddy Simulation of the flow past a circular cylinder at sub to super-critical Reynolds numbers.

[7] B. Koo, J. Yang, S.M. Yeon, F. Stern, Int. Journal Arch. Ocean Eng. 6, 2014, pp529-561. Reynolds and Froude number effect on the flow past an interface-piercing circular cylinder.

[8] T. Kawamura, S. Mayer, A. Garapon, L. Sorensen, Journal of Fluid Engineering, ASME, 2002. Large Eddy Simulation of a flow past a free surface piercing circular cylinder.

[9] X. Xiao, T. Tezdogan, A. Incecik, Techno-Ocean (2016), pp618-623. Numerical study on wave run-up height and depression depth around a vertical circular cylinder at various Froude numbers.

[10] H.G. Weller, G. Tabor, H. Jasak, C. Fureby, A tensorial approach to computational continuum mechanics using object-oriented technics, Computers in Physics 12(6), 1998

[11] F.R. Menter, AIAA Journal, 32 (8): 1598–1605, 1994. Two-Equation Eddy-Viscosity Turbulence Models for Engineering Applications.

[12] A.D. Hay, Princeton Univ., 1947, Princeton. Flow about semi-submerged cylinders of finite length.

[13] S M Yeon, J. Wang, F. Stern, Applied Ocean Research 59, 2016, pp 663-675. Large Eddy Simulation of the flow past a circular cylinder at sub to super-critical Reynolds numbers.

[14] AST Conway, D. Ranmuthugala, J.R. Binns, M. Renilson, Journal of Engineering for the maritime environment, 2017, pp1-13. The effect of geometry on the surface waves generated by vertical surface-piercing cylinders with a horizontal velocity.